Original Article

Genomic dissection of gastrointestinal and lung neuroendocrine neoplasm

Haixing Wang[1*], Li Sun[2*], Hua Bao[3*], Ao Wang[3], Panpan Zhang[4], Xue Wu[3], Xiaoling Tong[3], Xiaonan Wang[5], Jie Luo[6], Lin Shen[4], Yang W. Shao[3,7], Ming Lu[4]

[1]Department of Endoscopy Center, The First Affiliated Hospital of Xiamen University, Xiamen 361003, China; [2]Key Laboratory of Carcinogenesis and Translational Research (Ministry of Education/Beijing), Department of Pathology, Peking University Cancer Hospital & Institute, Beijing 100142, China; [3]Translational Medicine Research Institute, Geneseeq Technology Inc., Toronto M5G 1L7, Canada; [4]Key Laboratory of Carcinogenesis and Translational Research (Ministry of Education/Beijing), Department of Gastrointestinal Oncology, Peking University Cancer Hospital & Institute, Beijing 100142, China; [5]Medical Department, Nanjing Geneseeq Technology Inc., Nanjing 210032, China; [6]Department of Pathology, China-Japan Friendship Hospital, Beijing 100029, China; [7]School of Public Health, Nanjing Medical University, Nanjing 210029, China
*Those authors contributed equally to this work.
Correspondence to: Dr. Ming Lu. Key Laboratory of Carcinogenesis and Translational Research (Ministry of Education/Beijing), Department of Gastrointestinal Oncology, Peking University Cancer Hospital Institute, No. 52 Fucheng Road, Haidian District, Beijing 100142, China. Email: minglupku@163.com; Dr. Yang W. Shao. Translational Medicine Research Institute, Geneseeq Technology Inc., Suite 200, MaRS Center, South Tower, 101 College Street, Toronto, M5G 1L7, Canada. Email: yang.shao@geneseeq.com.

Abstract

Objective: Neuroendocrine neoplasms (NENs) are relatively rare and heterogeneous malignancies with two major subtypes: low-grade neuroendocrine tumor (NET) and high-grade neuroendocrine carcinoma (NEC). Comprehensive molecular characterization of NENs is needed to refine our understanding of the biological underpinnings of different NEN subtypes and to predict disease progression more accurately.

Methods: We performed whole-exome sequencing (WES) of NEN samples from 49 patients (25 NETs and 24 NECs) arising from the stomach, intestines or lung. Clinicopathologic features were assessed and associated with molecular events.

Results: NENs generally harbor a low mutation burden, with *TP53* being the top mutated gene found in 31% of patients. Consistent with other studies, p53 signaling pathway dysfunction is significantly enriched in NECs compared to NETs (P<0.01). Other than *TP53*, tissue type-specific mutation profiles of NENs were observed in our cohort compared to those reported in pancreatic NETs. Importantly, we observed significant genomic instability, with increased copy number alterations observed across the NEN genome, which was more profound in NECs and independently correlated with poor overall survival (OS) (P<0.001). NECs could be further stratified into two molecular subtypes based on OS (P<0.001) and the chromosomal instability score (CIS). Interestingly, we discovered that the gain of whole chromosome 5 occurred at the early stage of NEN development, followed by the loss of 5q exclusively in NECs (P<0.001).

Conclusions: These findings provide novel insights into the molecular characteristics of NENs and highlight the association of genomic stability with clinical outcomes.

Keywords: Neuroendocrine carcinoma; whole-exome sequencing; chromosomal instability

Submitted Jun 22, 2019. Accepted for publication Nov 27, 2019.
doi: 10.21147/j.issn.1000-9604.2019.06.08
View this article at: https://doi.org/10.21147/j.issn.1000-9604.2019.06.08

Introduction

Neuroendocrine neoplasms (NENs) are rare, heterogeneous malignancies that are steadily rising in both prevalence and incidence (1). Due to the body-wide distribution of neuroendocrine cells, NENs can originate from various organs, with most primary cases occurring in the gastrointestinal track and the bronchopulmonary system (1,2). In 2010, the revised World Health Organization (WHO) classification of NENs defined three grades based on the mitotic count and Ki-67 index (G1, G2, and G3) (3). In 2015, the National Comprehensive Cancer Network (NCCN) recommended the addition of tumor differentiation to NEN classification (4), which classified well-differentiated neoplasms as neuroendocrine tumors (NETs, G1 or G2) and poorly differentiated neoplasms as neuroendocrine carcinomas (NECs, G3). Studies have shown that NETs and NECs have distinct prognoses and responses to treatment (3,5), with pancreatic NETs (PanNETs) responding better to traditional chemotherapy than NECs (6). However, the histopathologic classification can be challenging due to the lack of well-defined histological criteria (7), and this dichotomization is far from perfect since some NETs are shown to behave like NECs (8). Furthermore, although NETs are mostly G1/G2 grade, regions of excessive proliferation comparable to G3 can also be found within NETs, which is associated with reduced disease-specific survival (9). This suggests that different molecular subtypes may exist within the same histological group, and current classification methods based on histology or the Ki-67 index may not adequately capture important differences at the molecular level.

To date, most genomic profiling studies on NENs have mainly focused on PanNETs and small intestine NETs (SI-NETs). It has been shown that *DAXX/ATRX*, *MEN1* and mTOR pathway genes are frequently altered in PanNETs (10-12). As a result, targeted therapy with the mTOR inhibitor everolimus has been reported to improve progression-free survival in advanced PanNET patients (13). Conversely, SI-NETs harbor relatively fewer recurrent mutations, with *CDKN1B* being the most commonly affected gene (14,15). However, less is known about the genomic landscapes in high-grade NECs or NENs arising from other anatomical sites (i.e., the stomach and lung). Poorly differentiated NECs are aggressive cancers with few treatment options. One recent study utilizing a 50-gene panel showed that *TP53*, *KRAS*, *PIK3CA/PTEN* and *BRAF* mutations were common in these NECs (11). Nevertheless, genomic data on NENs from sites other than the pancreas [nonpancreatic NENs (NP-NENs)] remain scarce, and additional comprehensive genome-wide studies are needed to fully elucidate their molecular characteristics and uncover novel therapeutic targets and prognostic markers. Here, we performed whole-exome sequencing (WES) on tumor samples and matched normal controls from 49 NP-NEN patients (29 in the stomach, 10 in the intestine, and 10 in the lung) for mutation profiling and somatic copy number alteration (SCNA) analysis, aiming to discover genomic signatures among distinct NEN subtypes and to identify potential biomarkers associated with clinical outcomes.

Materials and methods

Patient and sample overview

We retrospectively analyzed formalin-fixed paraffin-embedded (FFPE) tumor samples from 121 NEN patients treated at Peking University Cancer Hospital between 2012 and 2016, with consent signed by the patients or their legal guardians. Neuroendocrine features were confirmed by hematoxylin eosin (H&E) staining under light microscopy and immunohistochemistry (IHC) staining for neuroendocrine markers. Among these 121 tumor samples, 63 samples without matched normal control tissues and 9 low tumor purity (<30%) samples were excluded. The remaining 49 specimens from different tissues of origin (stomach, intestines and lung) were analyzed in this study. Each sample was assessed for the Ki-67 index, annotated G grade and differentiation (NET/NEC) based on independent pathologic evaluations by two pathologists. All NECs had a Ki67 index greater than 50%, consistent with previously reported findings (16,17). The detailed clinical information of all patients is included in *Supplementary Table S1*. The Ethics Committee of Peking University Cancer Hospital has reviewed and approved this study.

DNA isolation and library preparations

Genomic DNAs from FFPE sections were extracted with a QIAamp DNA FFPE Tissue Kit and quantified by Qubit 3.0 using the dsDNA HS Assay Kit (Thermo Fisher Scientific, Waltham, USA). Library preparations were performed with a KAPA Hyper Prep Kit (KAPA Biosystems, Wilmington, USA). Target enrichment was performed using the xGen Exome Research Panel v1.0 and Hybridization and Wash Reagents Kit (Integrated DNA Technology, Coralville, USA) according to the manufacturer's protocol. Sequencing was performed on an Illumina HiSeq 4000 platform using PE150 sequencing

chemistry (Illumina, San Diego, USA) to a mean coverage depth of 150× for tumor samples and 50× for matched normal control samples.

Sequencing data processing

Trimmomatic (18) was used for FASTQ file quality control. Leading/trailing low-quality reads (quality reading below 15) or N bases were removed. The high-quality reads were then aligned to the human reference genome (hg19) by BWA-MEM (19) with default parameters. Local realignment around indels and base quality score recalibration were performed with the Genome Analysis Toolkit (GATK 3.4.0).

Since loss of heterozygosity (LOH) is a common occurrence in cancer (20-22), allele-specific copy number (ASCN) analysis was performed with Fraction and Allele-Specific Copy Number Estimates from Tumor Sequencing (FACETS) (23) for the precise detection and separation of amplifications, deletions and LOH. The segmented ASCN results were then mapped to human genes based on their genomic coordinates. The ASCNs of major and minor alleles from the normal control sample were assumed as one copy. For each gene, the Euclidean distance of ASCN between paired tumor and normal samples was calculated as follows:

$$\sqrt{(\text{majorASCN}-1)^2+(\text{minorASCN}-1)^2}$$

The overall chromosomal instability score (CIS) for each tumor sample was defined as the arithmetic average of Euclidean distances across all genes. Stomach samples were then clustered into two groups with the K-means algorithm, and the grouping criteria were extrapolated to categorize intestine and lung samples.

Genomic Identification of Significant Targets in Cancer (GISTIC) 2.0 (24) was used to identify significantly amplified and deleted focal- and arm-level landscape of somatic copy number alterations (SCNAs). Arm-level gain and loss were defined as log2 depth ratios >0.2 and <−0.2, respectively. Focal-level amplification and deletion were defined as log2 depth ratios >0.4 and <−0.4, respectively. Segments with 0 minor copy number were defined as LOH.

Somatic single-nucleotide variants (SNVs) were identified using MuTect (25), and small insertions and deletions (indels) were detected using SCALPEL (26). SNV and indel annotation was performed by ANNOVAR (Version 20180603, http://annovar.openbioinformatics.org/en/latest/). Common single nucleotide polymorphisms (SNPs) were removed if they were found in public databases (Exome Variant Server, 1,000 Genomes Project and Exome Aggregation Consortium) at a frequency >1%. In the somatic analysis, we considered only nonsynonymous, stop-gain SNVs and frameshift/nonframeshift indels. A mutation significance analysis was carried out using the MutSig2CV algorithm (27), as elaborated in The Cancer Genome Atlas (TCGA) project. Significantly mutated genes were identified based on a $P<0.01$.

Statistical analysis

Fisher's exact test was used to analyze categorical variables in the contingency table. The Wilcoxon rank-sum test was used to find associations between categorical and numerical variables. The association between overall survival (OS) and chromosomal instability (CIN) was analyzed using the Kaplan-Meier method and compared by log-rank tests with the R packages *survival* and *survminer*. The multivariate analysis was performed using Cox regression, controlling for age, sex, and histology subtypes. Oncoplots were drawn with *Complexheatmap*. Two-sided $P<0.05$ were considered significant. All statistical analyses were performed with R software (Version 3.3.3; R Foundation for Statistical Computing, Vienna, Austria).

Results

Patient overview and clinical characteristics

The patients' clinical information and tumor characteristics involved in this study are summarized in *Table 1*, with detailed information listed in *Supplementary Table S1*. The patients' ages ranged from 27 to 81 years old, with a median of 61 years old. The male to female ratio was 1.45:1, with significantly more male patients having NECs (83.3%) than NETs (36.0%) ($P=0.001$, Fisher's exact test). Stage I–IV NENs diagnosed at different anatomical sites, including the stomach (n=29), lung (n=10) and intestines (n=10), were collectively termed NP-NENs. Notably, all lung NENs were histologically classified as small cell NECs in our cohort, while intestinal NENs were exclusively NET phenotypes. Equal distributions of NETs (n=15) and NECs (n=14), as well as small cell (n=6) and large cell (n=7) phenotypes within NECs, were observed at the stomach. All NEC samples were G3 grade, with a Ki67 index >50%, while NETs contained samples from G1 to G3. We separated the lung and intestine samples from the stomach samples when testing for associations between genetic alterations and clinical characteristics or survival.

Table 1 Patients' clinical information and tumor characteristics

Characteristics	Total (n=49) [n (%)]	NET (n=25) [n (%)]	NEC (n=24) [n (%)]	P
Age at diagnosis (year)				0.003
<60	21 (42.9)	17 (68.0)	4 (16.7)	
≥60	27 (55.1)	7 (28.0)	20 (83.3)	
Unknown	1 (2.0)	1 (4.0)	0 (0)	
Median (range)	61 (27–81)	53 (27–81)	65 (47–79)	
Gender				0.001
Female	20 (40.8)	16 (64.0)	4 (16.7)	
Male	29 (59.2)	9 (36.0)	20 (83.3)	
Stages at diagnosis				<0.001
I	17 (34.7)	11 (44.0)	6 (25.0)	
II	6 (12.2)	2 (8.0)	4 (16.7)	
III	17 (34.7)	3 (12.0)	14 (58.3)	
IV	9 (18.4)	9 (36.0)	0 (0)	
Sites				<0.001
Lung	10 (20.4)	0 (0)	10 (41.7)	
Stomach	29 (59.2)	15 (60.0)	14 (58.3)	
Intestines	10 (20.4)	10 (40.0)	0 (0)	
G grade				<0.001
G1	4 (8.2)	4 (16.0)	0 (0)	
G2	17 (34.7)	17 (68.0)	0 (0)	
G3	28 (57.1)	4 (16.0)	24 (100)	
Histological diagnosis				–
NEC	24 (49.0)	–	–	
Small cell	–	–	16 (66.7)	
Large cell	–	–	7 (29.2)	
Mixed	–	–	1 (4.2)	
NET	25 (51.0)	–	–	

NET, neuroendocrine tumor; NEC, neuroendocrine carcinoma.

Mutational signature profile

In this cohort of NP-NENs, the most frequent nucleotide substitutions were the C:G > T:A transition (46.7%), the C:G > A:T transversion (18.0%), and the T:A > C:G transition (14.2%). In PanNENs (12), the C:G > T:A transition (42.3%), the T:A > C:G transition (16.3%), and the C:G > A:T transversion (15.8%) were the top 3 substitution types. Therefore, NP-NENs and PanNENs displayed similar patterns of single nucleotide substitution. Among the 30 mutational signatures classified on Catalogue Of Somatic Mutations In Cancer (COSMIC), the most prominent ones in this NP-NEN cohort were signature 1 (34.6%) which was associated with aging, and signature 3 (15.4%) which was associated with DNA double-strand break-repair dysfunction. Notably, signature 3 was also linked with germline and somatic mutations in BRAC1 and BRAC2. Similarly, these two signatures were the dominant types in PanNENs but occurred with reduced frequencies of 16.0% and 11.4%, respectively. On the other hand, notably increased signatures in PanNENs included signature 13 (4.1% *vs.* 2.0%), signature 16 (3.9% *vs*. 0.2%), and signature 19 (3.6% *vs*. 0.2%). The average proportions of each signature in NP-NENs and PanNENs are summarized in *Supplementary Table S2*.

Somatic mutations in NP-NENs

Frequently somatically mutated genes reoccurring in more than three patients in this NP-NEN cohort as well as previously reported PanNEN-associated genes [*TSC2*, *MEN1*, *ATRX*, *RB1*, *CDKN2A*, *BRAF*, *SETD2*, *MUTYH*,

PTEN, *TSC1*, *VHL* and *DEPDC5* (12)] are shown in *Figure 1*. In total, we observed different mutation profiles of NP-NENs compared to PanNENs. Somatic mutations in *MEN1* have been reported in ~35% of PanNENs (12,28). However, only three patients (6%; two NETs and one NEC from the stomach) in this cohort had *MEN1* somatic mutations. Other frequently mutated PanNEN-related genes (10) also occurred at a much lower frequency in our cohort, including *ATRX* (n=3), *SETD2* (n=2), *PTEN* (n=1), and *DEPDC5* (n=1). On the other hand, consistent with previous reports (11), the tumor suppressor gene *TP53* was the most frequently mutated gene (31% of patients) and was specifically enriched in NECs (58.3% *vs.* 4.0%, P<0.001, Fisher's exact test) (*Figure 1*). Considering that all intestinal samples were NETs and all lung samples were NECs, we further analyzed the distribution of *TP53* mutations in stomach samples and confirmed that it is indeed enriched in NECs (64.0% *vs.* 7.0%, P=0.002, Fisher's exact test). The retinoblastoma (RB) pathway is often inactivated in high-grade small cell NENs, although a variable prevalence of the *RB1* mutation has been reported (29,30). We identified *RB1* loss-of-function

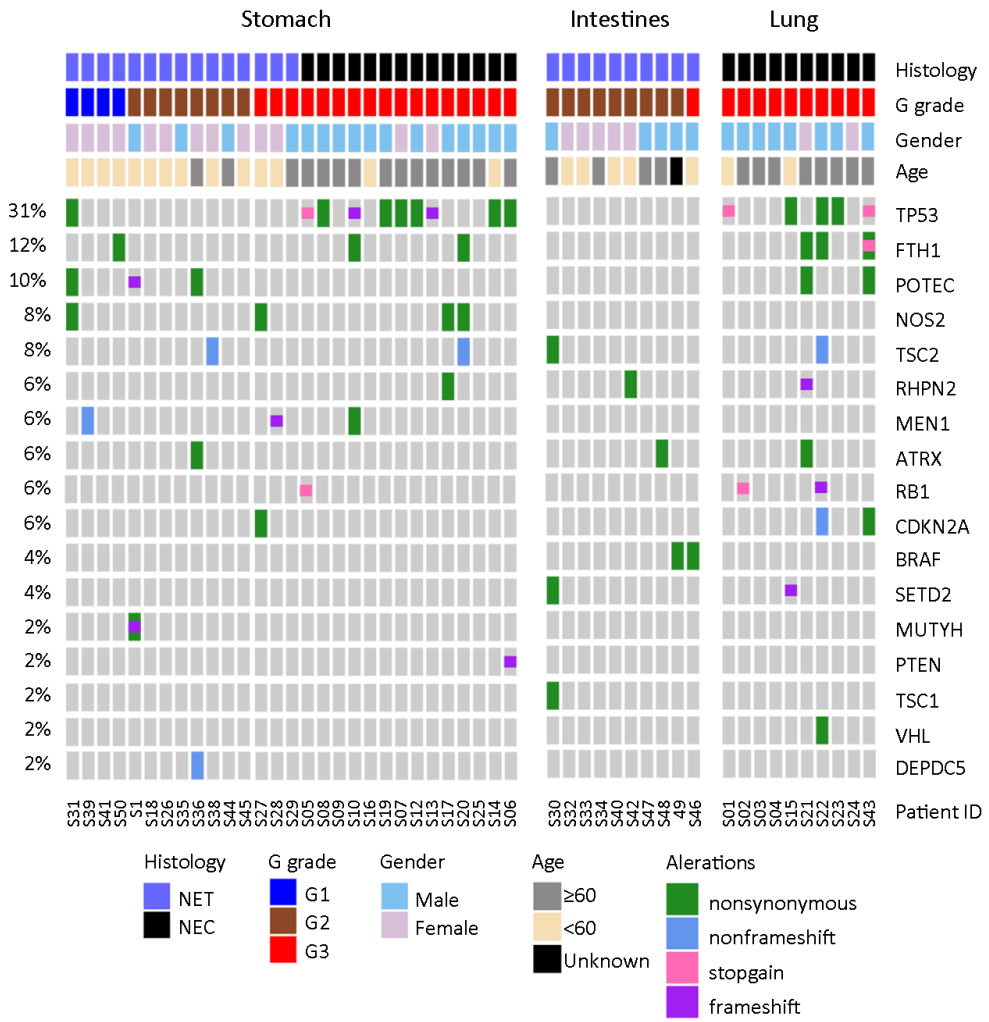

Figure 1 Somatic mutations identified in neuroendocrine neoplasms (NENs) of stomach, intestine and lung. Somatic mutation profiles of 49 NEN patients characterized by whole-exome sequencing (WES) analyses. The top panel indicates five different clinical characteristics of each patient, with the patient's ID and color coding labeled at the bottom. Samples were grouped based on anatomic sites (stomach, intestine and lung), histology [neuroendocrine tumor (NET)/neuroendocrine carcinoma (NEC)], and G grade (G1/G2/G3). The comutation matrix represents significantly mutated genes identified by MutSig2CV and previously reported pancreatic NEN-associated genes.

mutations in two small cell NEC samples of the lung and in one stomach small cell NEC within this cohort. Additional frequently mutated genes in this cohort included *FTH1* (a potential prognostic marker in breast cancer) (31), *POTEC* (a tumor subtype-specific cancer-testis antigen) (32), and *NOS2* (dual roles reported in tumorigenesis) (33). *FTH1* mutations also had a trend of higher prevalence in NEC samples. Furthermore, the mTOR pathway genes *TSC1/TSC2* were collectively mutated in 8% of the tumors. $BRAF^{V600E}$ was previously reported in colorectal/gastroenteropancreatic NENs (34,35), and here we identified this mutation in two intestinal NET patients (*Figure 1*). The frequencies of common somatic mutations and LOH reported in PanNENs and in our NP-NEN cohort are summarized in *Supplementary Table S3*.

Landscape of SCNAs

SCNA events were frequently observed in NETs of different organ-specific origins (36,37). To further refine the landscape of SCNAs in NP-NENs and identify common patterns of genomic alterations among different organ types, we examined SCNAs in all 49 samples. Overall, NP-NEN samples, especially NECs, displayed complex SCNAs, with numerous gains, losses, and LOHs observed in almost all chromosomes (*Figure 2A*). GISTIC2 analysis identified 4 significant recurrent (Q<0.01) focal-level SCNA events (*Figure 2B*, *Figure 3A*, top panel): amplifications of 19q12 (Q<0.01, 27% of patients, containing the *CCNE1* gene), deletions of 13q14.2 (Q<0.001, 35% of patients, containing the *RB1* gene), 10q23.2 (Q<0.001, 31% of patients, containing the *PTEN* gene), and 9q21.11 (Q<0.01). At the chromosomal arm level, five gains and eight losses were found as significantly recurrent SCNAs (GISTIC2 Q<0.05, *Figure 3A*, middle panel). Importantly, SCNAs in these regions encompass well-known tumor-related genes such as *EGFR* (7p), *NRAS* (1q), *TP53* (17p), *APC* (5q), *BRCA1* and *RB1* (13q). Among these arm-level events, 10q loss, 20q gain and 7p gain were also reported in PanNENs (38) (*Supplementary Table S4*). However, other high frequency events in PanNENs, such as 11p and 11q loss as well as 7q and 17q gain, occurred in fewer NP-NEN patients.

Association between SCNAs and patients' clinicopathologic characteristics

First, we examined the association between recurrent

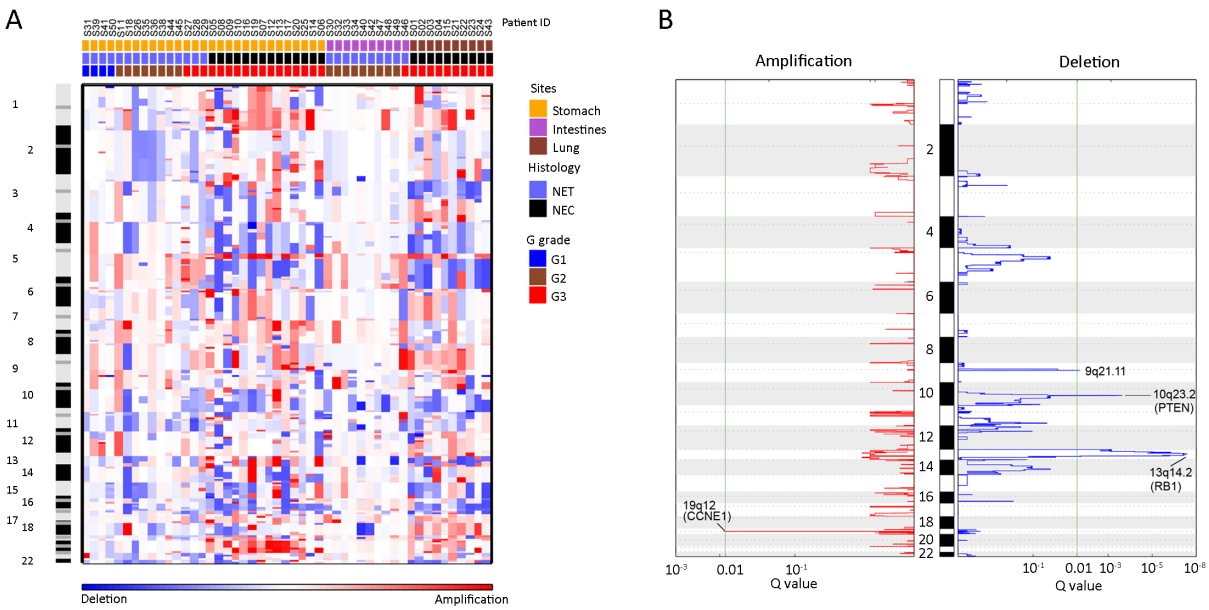

Figure 2 Landscape of arm- and focal-level somatic copy number alterations (SCNAs) in neuroendocrine neoplasms (NENs). (A) Heat map of arm-level copy number gains (red) and losses (blue) of 49 NEN tumor samples across the whole genome, ordered by site, histology, and G grade. Each column represents one patient. Chromosome numbers were labeled from top to bottom; (B) Significant recurrent focal-level copy number gains (red) and losses (blue) identified by Genomic Identification of Significant Targets in Cancer (GISTIC) 2.0. The false discovery rate (Q value) is plotted at the bottom. A Q value less than 0.01 (green line) is considered significant, and significantly altered focal loci are labeled.

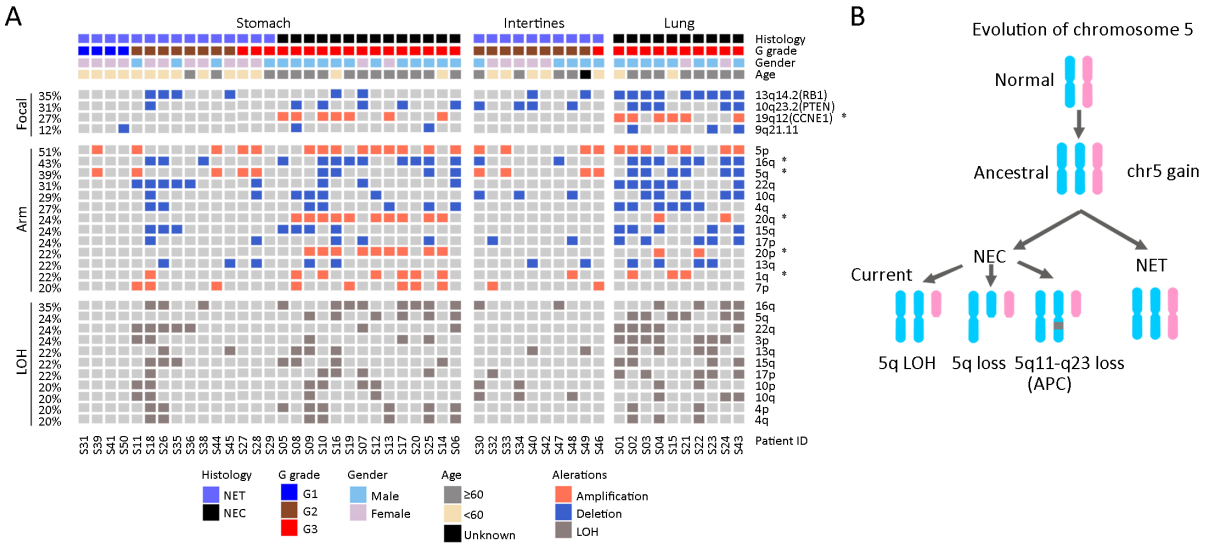

Figure 3 Recurrent arm- and focal-level somatic copy number alteration (SCNA) events in neuroendocrine neoplasms (NENs). (A) Distribution of recurrent arm- and focal-level SCNA events. Clinical characteristics were labeled for each patient, as indicated on the top. Top panel: significant focal-level (GISTIC2, Q<0.01) gains (orange) and losses (blue). Middle panel: significant arm-level (GISTIC2, Q<0.05) gains (orange) and losses (blue). Bottom panel: recurrent (≥20% of patients) arm-level losses of heterozygosity (LOH) (dark gray). * denotes significantly enriched events in neuroendocrine carcinomas (NECs) within the stomach cohort and the entire cohort; (B) A flowchart outlines the evolutionary pattern of chromosome 5 during NEN tumorigenesis. Two homologous chromosomes are represented as different colors, and the dark gray box indicates focal-level loss.

SCNAs and clinicopathologic characteristics in the stomach cohort. Amplifications in chromosome 19q12 (*CCNE1*), 20q, 20p, and 1q as well as deletion in 16q were significantly associated with NECs, while amplification in 5q was found exclusively within NETs (P<0.05, Fisher's exact test, *Table 2*, *Figure 3A*). These patterns were reaffirmed in the intestine and lung samples, as chromosome 19q12 (*CCNE1*), 20q and 20p amplifications were exclusively found in lung NECs, while 5q amplification was observed only in intestine NETs. In addition, *CCNE1* belongs to the p53 signaling pathway and is frequently overexpressed in various cancers (39,40). In the entire cohort, 23/49 (47%) patients had either a *TP53* mutation or *CCNE1* amplification, and only one patient had NET histology. Together, these results indicate that p53 signaling pathway dysfunction is a potential molecular characteristic of the NEC subtype of NENs.

Interestingly, in stomach samples, chromosome 5q amplification was exclusively associated with NETs (5/5), while 5q deletion was found only in NECs (4/4). Further examination showed that all 5q alterations cooccurred with 5p amplification. The same pattern was observed in the intestine and lung samples (*Figure 3A*). Furthermore, although some NEC samples showed 5p gain but not 5q loss, they all harbored a significant segment loss of 5q11-q23 (containing tumor suppressor genes such as *APC* and *MAP3K1*, data not shown). Therefore, there is a strong correlation between 5p and 5q arm abnormalities. One possible evolutionary route that may have led to the observed chromosome 5 alteration pattern is that copy number gain of the entire chromosome occurred first during the early stage of NEN tumorigenesis, followed by the loss of 5q or segments of 5q containing tumor suppressor genes that induced the transition from NEN to NEC (*Figure 3B*).

CIN and patients' clinical outcomes

In addition to individual SCNA events, the analysis of genome-wide chromosomal alterations and aneuploidy provides a holistic view of tumor genomic instability. To quantitatively assess the extent of whole-genome copy number abnormalities, we calculated the CIS for each tumor sample, which is defined as the average ASCN distance from all sequenced genes between paired tumor and normal control samples. A bimodal distribution of the CIS among all 49 patients was observed, suggesting the existence of two distinct clusters (*Supplementary Figure S1A*). In the stomach cohort, the K-means classifying algorithm produced two clusters, with 20 (69%) samples as

Table 2 SCNAs events significantly associated with NET or NEC

Events	Total			Stomach		
	NEC	NET	P	NEC	NET	P
20q amp	12	0	<0.001	10	0	<0.001
20p amp	11	0	<0.001	9	0	<0.001
19q12. Amp (CCNE1)	13	0	<0.001	7	0	0.002
5q amp	0	9	0.002	0	5	0.007
16q del	16	5	0.001	9	3	0.025
1q amp	9	2	0.018	6	1	0.035

SCNA, landscape of somatic copy number alteration; NET, neuroendocrine tumor; NEC, neuroendocrine carcinoma; Fisher's exact test were performed to identify association in all tissue types as well as in stomach samples alone.

the chromosomal stable (CS) group and 9 (31%) samples as the CIN group (*Supplementary Figure S1B*). The cut-off CIS value was 1.1. The same cut-off value was applied to the overall cohort, which generated very similar proportions between CS and CIN (67% *vs*. 33%). Overall, NECs consisted of both CS and CIN tumors (10 *vs*. 14), while all NETs were of the CS status (*Figure 4A*,*B*). The ASCN plots from samples representative of the CS and CIN groups are visualized at the genomic scale in *Supplementary Figure S2A*,*B*, respectively. Notably, tumor ploidy and tumor mutation burden (TMB) were also significantly higher in CIN tumors compared to CS tumors (P<0.01, Wilcoxon rank-sum test; *Supplementary Figure S2C*,*D*). Together, these results suggest that the development of NEC took distinct evolutionary trajectories, illustrated by the significantly more altered genome in NECs, with dysfunction in the p53 pathway, chromosome 5 amplification and 5q deletion (*Figure 4C*).

Next, we tested the potential association between genomic instability and patients' clinical outcomes. To reduce the bias of newly diagnosed patients with a limited follow-up, only noncensored patients or patients with at least 24 months of follow-up (12 stomach, 6 lung, and 5 intestine samples) were included in the analysis. Among the 12 stomach NEN patients, the CIN group showed significantly worse OS compared to the CS group (P=0.003, log-rank test, *Figure 5A*). In all tissue types of 23 patients, the same result was observed (P<0.001, log-rank test, *Figure 5B*). Although the difference was not significant when examined only in the lung cohort (P=0.162, log-rank test), the median OS of the CIN group was only 8 months compared to that of the CS group (not reached). A larger sample size will likely produce a significant correlation. When patients were further stratified by both CIN and histology, CIN-NEC patients had significantly reduced OS compared to both CS-NET and CS-NEC patients (P=0.013 in the stomach only; P<0.001 in all tissue types of 23 patients, log-rank test, *Figure 5C*,*D*). Furthermore, when the cohort was stratified by gender, age, grade, or stage, CIN tumors were associated with reduced OS in all groups (P<0.05, log-rank test, *Supplementary Figure S3*). After controlling for histology, gender, and age, CIN was the only factor associated with OS in all 23 patients (*Supplementary Table S5*).

Discussion

To date, all categorization methods of NENs are based on proliferative marker measurements or a histological evaluation by a pathologist. However, it is increasingly evident that neither method can fully distinguish clinically favorable tumors from aggressive carcinomas. Therefore, the genomic profiling of NENs can supplement the current categorization system to better predict survival and guide treatment decisions. Most previous genomic studies of NENs have focused on the relatively more frequent PanNETs or SI-NETs and have often profiled a small set of genes (11). Data on clinically unfavorable NECs and NENs originating from other organs (NP-NENs) are limited. Thus, there is an urgent need to uncover new molecular drivers and subtypes within NP-NENs that correlate with the patient's clinicopathologic characteristics or survival.

In this study, we performed WES profiling of 49 NP-NENs from three different organ types for genomic profiling. NP-NENs and Pan-NENs had similar mutational signature patterns, which are closely associated with aging and dysfunction in the DNA double-strand break-repair mechanism. However, NP-NENs exhibited a distinct mutational landscape from that of PanNETs. The most common PanNEN-associated *MEN1* mutation (28) was found at a surprisingly low frequency in NP-NENs. On the other hand, the mTOR pathway was frequently

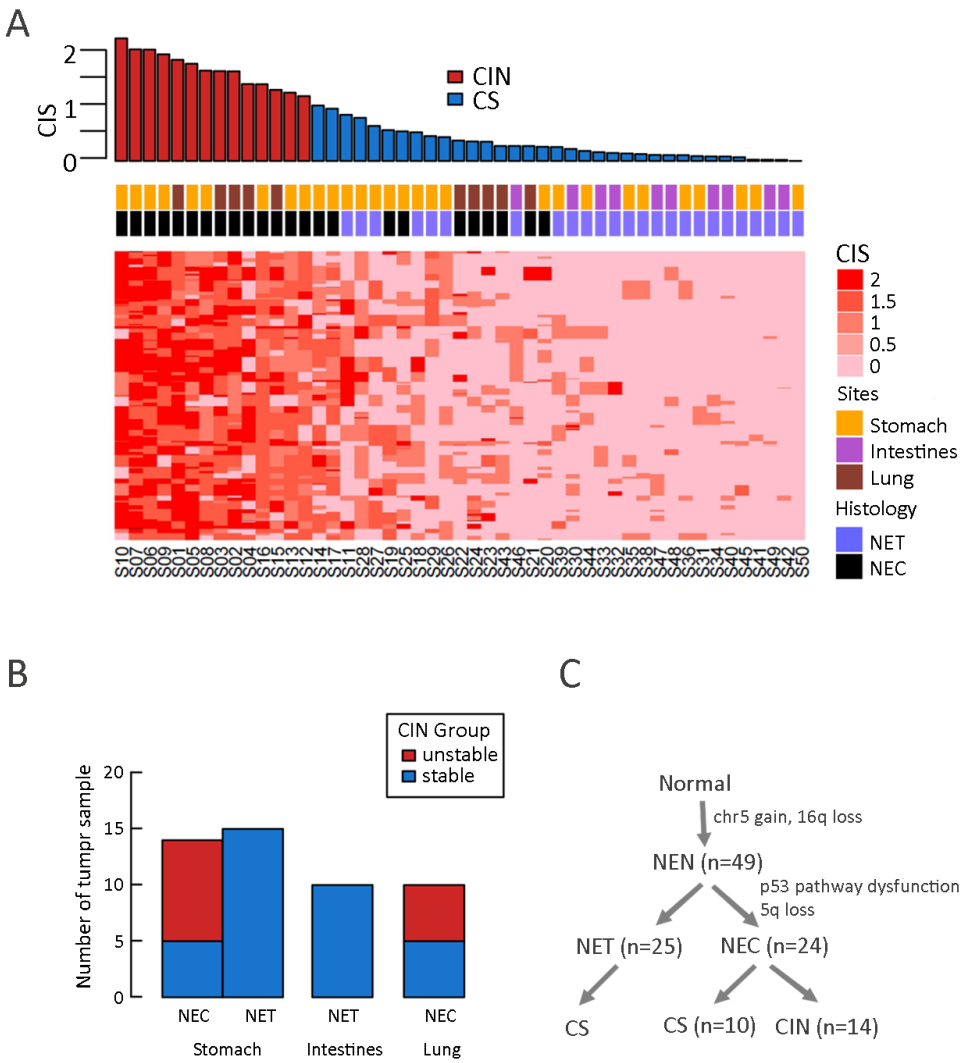

Figure 4 Chromosomal instability subtypes in nonpancreatic neuroendocrine neoplasms (NP-NENs). (A) Genome-wide chromosomal instability score (CIS) based on all protein-coding genes. The top panel shows the distribution of the CIS among 49 patients in descending order. Patients were classified as chromosomal stable (CS, blue) or chromosomal instability (CIN, red) using k-means in the R package. The CIS matrix was constructed by presenting the CIS of each individual gene; (B) Distribution of the CS and CIN subtypes across three clinical characteristics (histology, tissue site and G grade); (C) A flowchart outlines how NEN tumors were classified into different molecular subtypes. NET, neuroendocrine tumor; NEC, neuroendocrine carcinoma.

altered in PanNETs (12). Here, we also observed a considerable degree of aberration in genes of this pathway in NP-NENs. RB1 loss of function is commonly reported in small cell NENs (30), and we observed both mutation and copy number loss in RB1 in patients with small cell NEC of the lung. Additionally, we discovered that genes not previously linked to NENs occurred at considerable frequencies in our cohort, such as *FTH1*, *POTEC*, and *NOS2*. Finally, consistent with previous reports, *TP53* was the most frequently mutated gene and was associated with poorly differentiated NECs (11,30,41). These results suggest that NP-NENs and PanNENs have different mechanisms of tumorigenesis.

Compared to the low mutation burden in NP-NENs, our study revealed extensive focal- and arm-level SCNAs in NENs, especially in NECs. The gain of chromosome 5 was previously identified as a common feature in gastrointestinal NETs (42), and the loss of 5q was reported in lung NECs (43). Here, we observed chromosome 5 gain in both NETs and NECs, but only NECs underwent

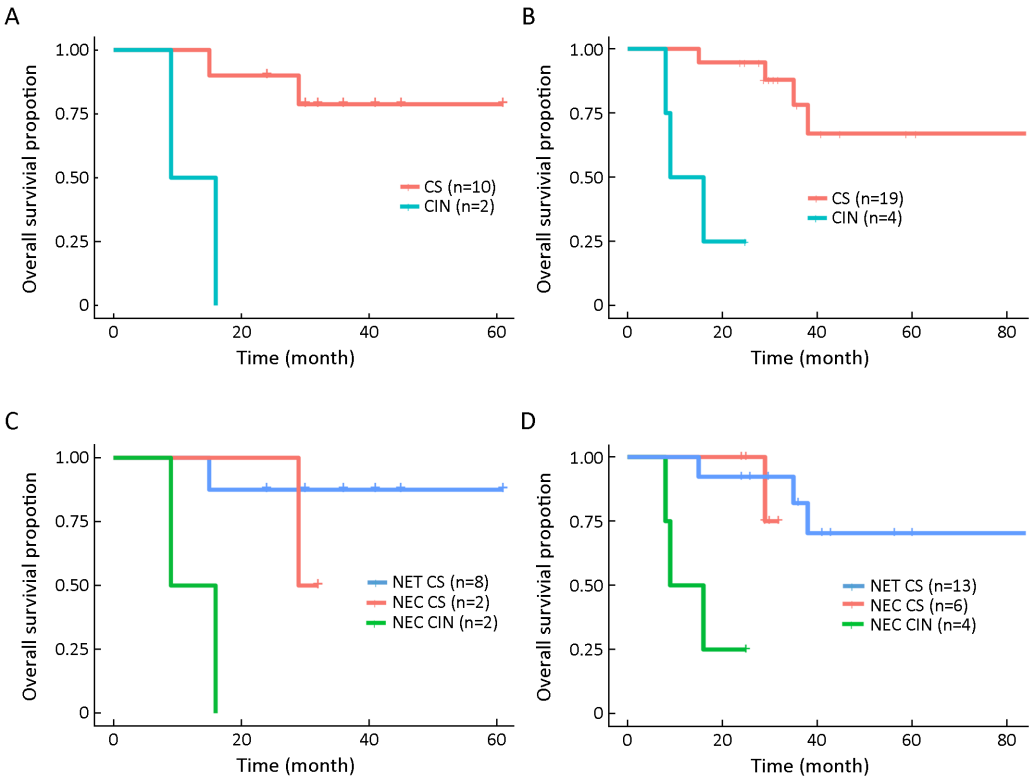

Figure 5 Distinction of overall survival (OS) between chromosomal instability (CIN) and chromosomal stable (CS) patients. Patients were included in the analysis if the follow-up time was longer than 24 months or if death occurred. Kaplan-Meier plot of OS between CIN and CS patients in the stomach neuroendocrine neoplasm (NEN) cohort (P=0.003) (A) and in all tissue types (P<0.001) (B); Kaplan-Meier plot when patients were stratified by both the chromosomal instability score (CIS) and histology type in the stomach only (P=0.013) (C) and in all tissue types (P<0.001) (D). NET, neuroendocrine tumor; NEC, neuroendocrine carcinoma.

subsequent 5q deletion. This is potentially an important evolutionary mechanism of NEN tumorigenesis and a prerequisite of transformation from a clinically favorable NET subtype to a malignant NEC subtype (*Figure 4C*). Another distinct feature of NECs is chromosome 20 gain, which was also found to be associated with reduced survival in other studies (36).

CIS subtypes have been well characterized in colorectal and gastric cancers; however, they have not been reported in NENs. Our study investigated genome-wide chromosomal alterations in NENs and found that a proportion of NECs displayed extensive alterations in chromosome copy numbers. Specifically, NECs were further stratified into a CS group, which had comparable survival outcomes with NETs, and a CIN group, which had significantly reduced survival. However, our conclusion could be limited by the small sample size of patients with long-term survival data, which was further reduced in the stratified cohort analysis. Nonetheless, the diminished survival in the CIN group was observed across different clinical strata, suggesting its prognostic value. Future studies with large sample sizes are needed to fully validate the utility of CIS in NEN classification in conjunction with the Ki67 index and histology.

Conclusions

Our findings provide insights into the molecular and evolutionary characteristics of NENs and highlight the importance of differentiation between CIS subtypes and their associations with survival outcomes. We demonstrated that despite originating from different organs, NECs share remarkably similar genetic signatures. Future studies involving larger cohorts and diverse organ types are warranted to estimate the distribution of CIS in NENs and validate its prognostic value.

Acknowledgements

None.

Footnote

Conflicts of Interest: Hua Bao, Xue Wu, Ao Wang, Xiaoling Tong and Yang W. Shao are employees of Geneseeq Technology, Inc. Xiaonan Wang is an employee of Nanjing Geneseeq Technology, Inc. The authors have no conflicts of interest to declare.

References

1. Oronsky B, Ma PC, Morgensztern D, et al. Nothing but NET: A review of neuroendocrine tumors and carcinomas. Neoplasia 2017;19:991-1002.
2. Anaizi A, Rizvi-Toner A, Valestin J, et al. Large cell neuroendocrine carcinoma of the lung presenting as pseudoachalasia: a case report. J Med Case Rep 2015; 9:56.
3. Klöppel G. Classification and pathology of gastroenteropancreatic neuroendocrine neoplasms. Endocr Relat Cancer 2011;18 Suppl 1:S1-16.
4. Kulke MH, Shah MH, Benson AB 3rd, et al. Neuroendocrine tumors, version 1. 2015. J Natl Compr Canc Netw 2015;13:78-108.
5. Thomaz Araújo TM, Barra WF, Khayat AS, et al. Insights into gastric neuroendocrine tumors burden. Chi J Cancer Res 2017;29:137-43.
6. Strosberg JR, Fine RL, Choi J, et al. First-line chemotherapy with capecitabine and temozolomide in patients with metastatic pancreatic endocrine carcinomas. Cancer 2011;117:268-75.
7. Tang LH, Basturk O, Sue JJ, et al. A practical approach to the classification of WHO Grade 3 (G3) well-differentiated neuroendocrine tumor (WD-NET) and poorly differentiated neuroendocrine carcinoma (PD-NEC) of the pancreas. Am J Surg Pathol 2016;40:1192-202.
8. Nikou GC, Angelopoulos TP. Current concepts on gastric carcinoid tumors. Gastroenterol Res Pract 2012; 2012:287825.
9. Tang LH, Untch BR, Reidy DL, et al. Well-differentiated neuroendocrine tumors with a morphologically apparent high-grade component: A pathway distinct from poorly differentiated neuroendocrine carcinomas. Clin Cancer Res 2016; 22:1011-7.
10. Jiao Y, Shi C, Edil BH, et al. DAXX/ATRX, MEN1, and mTOR pathway genes are frequently altered in pancreatic neuroendocrine tumors. Science 2011; 331:1199-203.
11. Vijayvergia N, Boland PM, Handorf E, et al. Molecular profiling of neuroendocrine malignancies to identify prognostic and therapeutic markers: a Fox Chase Cancer Center Pilot Study. Br J Cancer 2016; 115:564-70.
12. Scarpa A, Chang DK, Nones K, et al. Whole-genome landscape of pancreatic neuroendocrine tumours. Nature 2017;543:65-71.
13. Yao JC, Shah MH, Ito T, et al. Everolimus for advanced pancreatic neuroendocrine tumors. N Engl J Med 2011;364:514-23.
14. Francis JM, Kiezun A, Ramos AH, et al. Somatic mutation of CDKN1B in small intestine neuroendocrine tumors. Nat Genet 2013;45:1483-6.
15. Banck MS, Kanwar R, Kulkarni AA, et al. The genomic landscape of small intestine neuroendocrine tumors. J Clin Invest 2013;123:2502-8.
16. Kidd M, Modlin I, Öberg K. Towards a new classification of gastroenteropancreatic neuroendocrine neoplasms. Nat Rev Clin Oncol 2016;13:691-705.
17. Vélayoudom-Céphise FL, Duvillard P, Foucan L, et al. Are G3 ENETS neuroendocrine neoplasms heterogeneous? Endocr Relat Cancer 2013;20:649-57.
18. Bolger AM, Lohse M, Usadel B. Trimmomatic: a flexible trimmer for Illumina sequence data. Bioinformatics 2014;30:2114-220.
19. Li H, Durbin R. Fast and accurate short read alignment with Burrows-Wheeler transform. Bioinformatics 2009;25:1754-60.
20. Peng HQ, Bailey D, Bronson D, et al. Loss of heterozygosity of tumor suppressor genes in testis cancer. Cancer Res 1995;55:2871-5.
21. Abdel Wahab AH, Abo-Zeid HI, El-Husseini MI, et al. Role of loss of heterozygosity on chromosomes 8 and 9 in the development and progression of cancer bladder. J Egypt Natl Canc Inst 2005;17:260-9.
22. Oesterreich S, Allredl DC, Mohsin SK, et al. High rates of loss of heterozygosity on chromosome 19p13 in human breast cancer. Br J Cancer 2001;84:493-8.
23. Shen R, Seshan VE. FACETS: allele-specific copy number and clonal heterogeneity analysis tool for high-throughput DNA sequencing. Nucleic Acids Res 2016;44:e131.
24. Mermel CH, Schumacher SE, Hill B, et al.

GISTIC2.0 facilitates sensitive and confident localization of the targets of focal somatic copy-number alteration in human cancers. Genome Biol 2011;12:R41.
25. Cibulskis K, Lawrence MS, Carter SL, et al. Sensitive detection of somatic point mutations in impure and heterogeneous cancer samples. Nat Biotechnol 2013; 31:213-9.
26. Fang H, Bergmann EA, Arora K, et al. Indel variant analysis of short-read sequencing data with Scalpel. Nat Protoc 2016;11:2529-48.
27. Lawrence MS, Stojanov P, Polak P, et al. Mutational heterogeneity in cancer and the search for new cancer-associated genes. Nature 2013;499:214-8.
28. Corbo V, Dalai I, Scardoni M, et al. MEN1 in pancreatic endocrine tumors: analysis of gene and protein status in 169 sporadic neoplasms reveals alterations in the vast majority of cases. Endocr Relat Cancer 2010;17:771-83.
29. Travis WD. Lung tumours with neuroendocrine differentiation. Eur J Cancer 2009;45 Suppl 1:251-66.
30. Vollbrecht C, Werner R, Walter RF, et al. Mutational analysis of pulmonary tumours with neuroendocrine features using targeted massive parallel sequencing: a comparison of a neglected tumour group. Br J Cancer 2015;113:1704-11.
31. Liu NQ, De Marchi T, Timmermans AM, et al. Ferritin heavy chain in triple negative breast cancer: a favorable prognostic marker that relates to a cluster of differentiation 8 positive (CD8+) effector T-cell response. Mol Cell Proteomics 2014;13:1814-27.
32. Yao J, Caballero OL, Yung WK, et al. Tumor subtype-specific cancer-testis antigens as potential biomarkers and immunotherapeutic targets for cancers. Cancer Immunol Res 2014;2:371-9.
33. Xu W, Liu LZ, Loizidou M, et al. The role of nitric oxide in cancer. Cell Res 2002;12:311-20.
34. Klempner SJ, Gershenhorn B, Tran P, et al. $BRAF^{V600E}$ mutations in high-grade colorectal neuroendocrine tumors may predict responsiveness to BRAF-MEK combination therapy. Cancer Discov 2016;6:594-600.
35. Park C, Ha SY, Kim ST, et al. Identification of the BRAF V600E mutation in gastroenteropancreatic neuroendocrine tumors. Oncotarget 2016;7:4024-35.
36. Hashemi J, Fotouhi O, Sulaiman L, et al. Copy number alterations in small intestinal neuroendocrine tumors determined by array comparative genomic hybridization. BMC Cancer 2013;13:505.
37. Zhao J, de Krijger RR, Meier D, et al. Genomic alterations in well-differentiated gastrointestinal and bronchial neuroendocrine tumors (carcinoids): marked differences indicating diversity in molecular pathogenesis. Am J Pathol 2000;157:1431-8.
38. Capurso G, Festa S, Valente R, et al. Molecular pathology and genetics of pancreatic endocrine tumours. J Mol Endocrinol 2012;49:R37-50.
39. Ayhan A, Kuhn E, Wu RC, et al. CCNE1 copy-number gain and overexpression identify ovarian clear cell carcinoma with a poor prognosis. Mod Pathol 2017;30:297-303.
40. Nakayama K, Rahman MT, Rahman M, et al. CCNE1 amplification is associated with aggressive potential in endometrioid endometrial carcinomas. Int J Oncol 2016;48:506-16.
41. Shao Y, Li X, Lu Y, et al. Aberrant LRP16 protein expression in primary neuroendocrine lung tumors. Int J Clin Exp Pathol 2015;8:6560-5.
42. Zikusoka MN, Kidd M, Eick G, et al. The molecular genetics of gastroenteropancreatic neuroendocrine tumors. Cancer 2005;104:2292-309.
43. Rossi G, Bertero L, Marchiò C, et al. Molecular alterations of neuroendocrine tumours of the lung. Histopathology 2018;72:142-52.

Cite this article as: Wang H, Sun L, Bao H, Wang A, Zhang P, Wu X, Tong X, Wang X, Luo J, Shen L, Shao YW, Lu M. Genomic dissection of gastrointestinal and lung neuroendocrine neoplasm. Chin J Cancer Res 2019;31 (6):918-929. doi: 10.21147/j.issn.1000-9604.2019.06.08

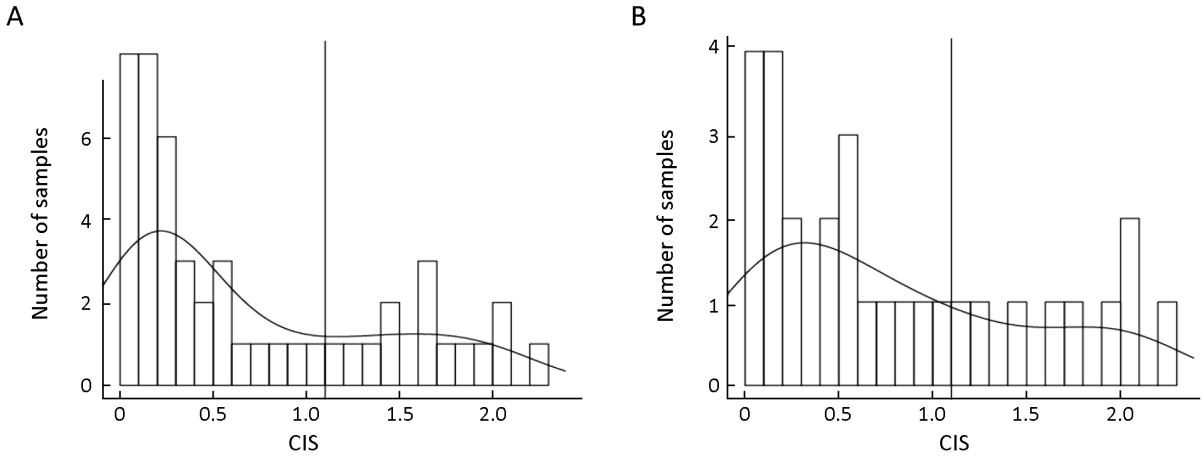

Figure S1 Distribution of chromosomal instability score (CIS) among all 49 neuroendocrine neoplasms (NENs) patients (A) and within the stomach cohort only (B). The K-means clustering algorithm separated patients into two groups. Samples to the left of the vertical line are chromosomal stable (CS) and samples to the right are chromosomal instability (CIN).

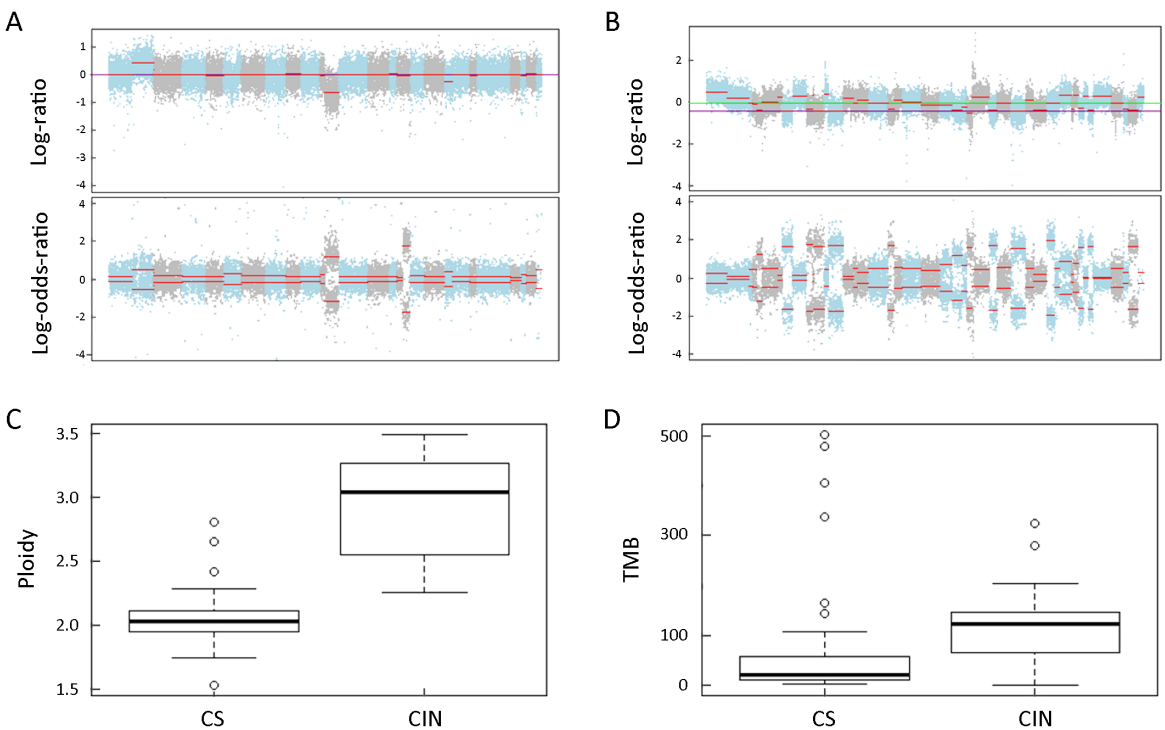

Figure S2 Ploidy and tumor mutation burden (TMB) difference between chromosomal instability (CIN) and chromosomal stable (CS) samples. Top panel: Fraction and Allele-Specific Copy Number Estimates from Tumor Sequencing (FACETS) results showing genome-wide log-ratio and log-odds-ratio of a CS tumor sample (A) and a CIN tumor sample (B); Bottom panel: boxplot of ploidy by CIS subtypes (P<0.001) (C) and TMB by CIS subtypes (P=0.004) (D).

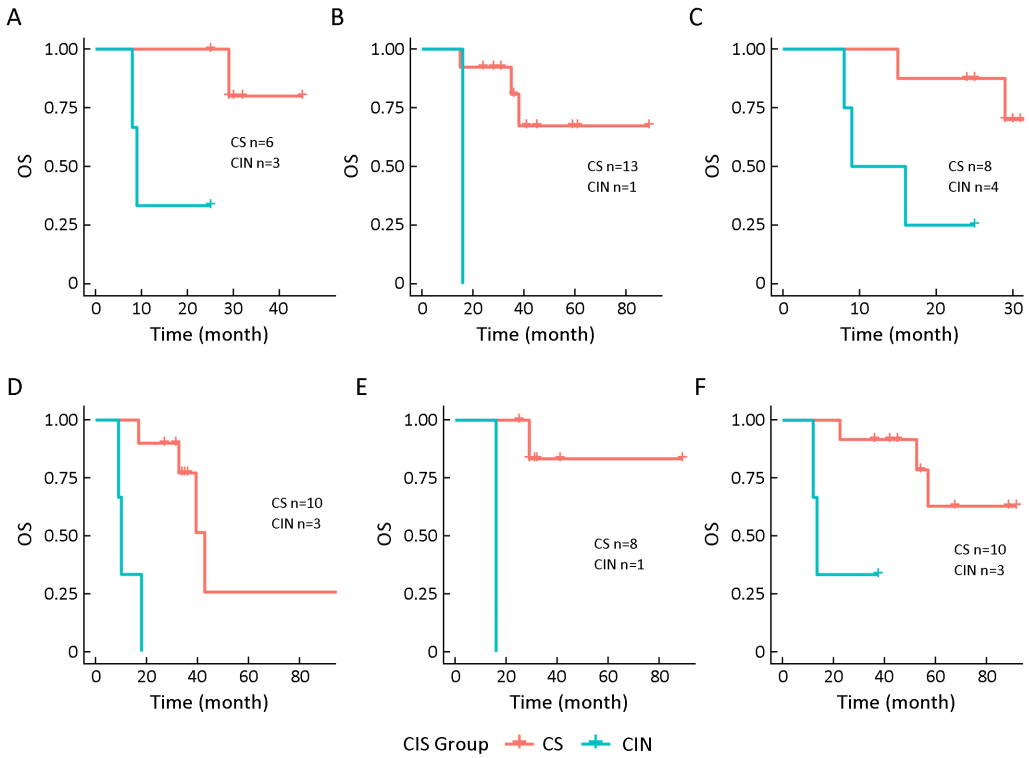

Figure S3 Stratified Kaplan-Meier analysis of survival difference between chromosomal instability (CIN) and chromosomal stable (CS) subtypes. Kaplan-Meier plot of overall survival (OS) between CIN and CS subtypes stratified by gender [male (A): P=0.027; female (B): P=0.022)], G grade [grade G3 (C): P=0.023], stage [stage III&IV (D): P<0.001] and age [median, 60.5 years old; age high (E): P=0.008; age low (F): P=0.008)].

Table S1 Clinical characteristics of each individual patient

Patient_ID	Gender	Age at diagnosis (year)	Stages at diagnosis	Sites	OS (month)	Death*	G_grade	Ki67_index (%)	Histological diagnosis	NEC cell type	CIN group	CIN index	Tumor content estimated by FACETS (%)	Ploidy
S01	Male	53	IA	Lung	25	0	G3	>75	NEC	Small	Unstable	1.8513	78.4	3.27
S02	Male	79	IIIB	Lung	22	0	G3	80	NEC	Small	Unstable	1.6406	68.8	2.97
S03	Male	62	IIIB	Lung	8	1	G3	90	NEC	Small	Unstable	1.6444	61.2	3.49
S04	Male	70	IB	Lung	17	0	G3	>75	NEC	Small	Unstable	1.4075	64.8	2.53
S05	Male	62	IIB	Stomach	10	0	G3	70	NEC	Small	Unstable	1.7795	51.2	3.24
S06	Male	71	IIIB	Stomach	6	0	G3	75	NEC	Large	Unstable	2.0379	60.6	3.08
S07	Female	64	IIIB	Stomach	7	0	G3	>75	NEC	Large	Unstable	2.0419	60.4	3.25
S08	Male	64	IIIB	Stomach	7	0	G3	70	NEC	Small	Unstable	1.6527	70.8	3.43
S09	Male	60	IIA	Stomach	4	0	G3	70	NEC	Small	Unstable	1.9519	48.8	2.90
S10	Male	60	IIIB	Stomach	9	1	G3	80	NEC	Small	Unstable	2.2426	87.4	3.23
S11	Male	47	I	Stomach	45	0	G2	5	NET	NA	Stable	0.8445	45.8	2.15
S12	Male	67	IIB	Stomach	23	0	G3	>75	NEC	Large	Unstable	1.1868	34.7	2.54
S13	Female	74	IIIB	Stomach	16	1	G3	80	NEC	Large	Unstable	1.2501	48.0	2.40
S14	Male	47	IIIB	Stomach	14	0	G3	>75	NEC	Mixed	Unstable	1.0149	68.8	2.57
S15	Male	59	IA	Lung	19	0	G3	>75	NEC	Small	Unstable	1.3014	35.0	3.01
S16	Male	50	IIIB	Stomach	3	0	G3	>80	NEC	Small	Unstable	1.4038	57.5	3.44
S17	Male	69	IIB	Stomach	9	0	G3	>75	NEC	Large	Unstable	0.9562	62.1	2.25
S18	Female	53	I	Stomach	45	0	G2	2–20	NET	NA	Stable	0.5248	64.0	1.80
S19	Male	72	IIIB	Stomach	29	1	G3	80	NEC	Small	Stable	0.5650	60.9	2.05
S20	Male	65	IIIB	Stomach	32	0	G3	>75	NEC	Large	Stable	0.2595	54.2	2.08
S21	Female	71	IIIB	Lung	31	0	G3	>75	NEC	Small	Stable	0.2730	87.9	2.42
S22	Male	68	IA	Lung	29	0	G3	>75	NEC	Small	Stable	0.3743	75.5	2.05
S23	Male	62	IA	Lung	1	0	G3	>75	NEC	Small	Stable	0.3517	77.5	1.76
S24	Female	61	IIIB	Lung	24	0	G3	>75	NEC	Small	Stable	0.3572	60.2	2.03
S25	Male	74	IIIB	Stomach	1	0	G3	50–75	NEC	Large	Stable	0.5418	62.5	1.75
S26	Female	52	I	Stomach	13	0	G2	5	NET	NA	Stable	0.4359	48.9	1.54
S27	Female	59	IV	Stomach	15	1	G3	30	NET	NA	Stable	0.6413	47.5	2.28
S28	Female	58	IV	Stomach	7	0	G3	32	NET	NA	Stable	0.7896	43.5	2.65
S29	Male	60	IIIB	Stomach	30	0	G3	30	NET	NA	Stable	0.4552	53.4	2.81
S30	Male	70	IIA	Intestines (rectum)	12	0	G2	10	NET	NA	Stable	0.2192	62.6	1.99

Table S1 (*continued*)

Table S1 (*continued*)

Patient_ID	Gender	Age at diagnosis (year)	Stages at diagnosis	Sites	OS (month)	Death*	G_grade	Ki67_index (%)	Histological diagnosis	NEC cell type	CIN group	CIN index	Tumor content estimated by FACETS (%)	Ploidy
S31	Female	44	I	Stomach	61	0	G1	1	NET	NA	Stable	0.0888	32.4	1.93
S32	Female	47	IV	Intestines (duodenum)	38	1	G2	10	NET	NA	Stable	0.1472	54.9	2.09
S33	Female	36	I	Intestines (duodenum)	59	0	G2	5	NET	NA	Stable	0.1615	36.3	2.11
S34	Female	79	IV	Intestines (rectum)	89	0	G2	5	NET	NA	Stable	0.0829	40.8	1.92
S35	Male	45	IIIB	Stomach	NA	0	G2	5	NET	NA	Stable	0.1377	47.9	1.91
S36	Female	67	I	Stomach	41	0	G2	6	NET	NA	Stable	0.1067	49.1	1.77
S38	Female	53	I	Stomach	5	0	G2	3	NET	NA	Stable	0.1261	49.3	1.96
S39	Female	40	I	Stomach	36	0	G1	1	NET	NA	Stable	0.2552	39.1	2.11
S40	Female	52	IV	Intestines (rectum)	35	1	G2	5	NET	NA	Stable	0.0813	84.8	1.96
S41	Female	59	I	Stomach	3	0	G1	1	NET	NA	Stable	0.0224	42.2	2.19
S42	Female	52	IV	Intestines (rectum)	28	0	G2	10	NET	NA	Stable	0.0196	70.1	2.06
S43	Male	65	IA	Lung	25	0	G3	75	NEC	Small	Stable	0.2736	82.3	2.01
S44	Male	81	IIIB	Stomach	NA	0	G2	5	NET	NA	Stable	0.1836	45.7	2.12
S45	Female	27	I	Stomach	21	0	G2	3	NET	NA	Stable	0.0681	45.2	2.13
S46	Male	50	IV	Intestines (duodenum)	12	0	G3	25	NET	NA	Stable	0.2735	57.5	2.15
S47	Male	70	IIA	Intestines (rectum)	12	0	G2	10	NET	NA	Stable	0.1100	38.0	1.95
S48	Male	68	IV	Intestines (sigmoid colon)	11	0	G2	10	NET	NA	Stable	0.1076	70.0	2.01
S49	Male	NA	IV	Intestines (rectum)	9	0	G2	20	NET	NA	Stable	0.0220	54.6	2.02
S50	Female	47	I	Stomach	24	0	G1	1	NET	NA	Stable	0.0000	69.1	1.97

OS, overall survival; NEC, neuroendocrine carcinoma; CIN, chromosomal instability; FACETS, Fraction and Allele-Specific Copy Number Estimates from Tumor Sequencing; NET, neuroendocrine tumor; NA, not available; *, 1=death, 0=no event; Sample from patient S37 was removed due to sample contamination.

Table S2 Mean proportion of 30 COSMIC mutational signatures in PanNENs and NP-NENs

COSMIC signature	Ref (12)	Our data
Signature.1	0.159982238	0.346228362
Signature.10	0.011079643	0.010392651
Signature.11	0.032256010	0.013738497
Signature.12	0.021285641	0.013442374
Signature.13	0.041404037	0.019918897
Signature.14	0.005894283	0.001727616
Signature.15	0.032758491	0.029411381
Signature.16	0.039199494	0.002234721
Signature.17	0.021933895	0.018716511
Signature.18	0.047276639	0.013247281
Signature.19	0.035502515	0.002246793
Signature.2	0.018432333	0.013873117
Signature.20	0.027670301	0.022180302
Signature.21	0.032648917	0.014806427
Signature.22	0.011832450	0.003458886
Signature.23	0.033268548	0.039591606
Signature.24	0.034368941	0.062426407
Signature.25	0.008030420	0.003873105
Signature.26	0.017426507	0.024303159
Signature.27	0.010720511	0.000851746
Signature.28	0.009624432	0.007964046
Signature.29	0.031873880	0.027362037
Signature.3	0.114408516	0.153535185
Signature.30	0.037531756	0.013375991
Signature.4	0.032605106	0.075485003
Signature.5	0.011852951	0.003172427
Signature.6	0.053626062	0.031599656
Signature.7	0.030288502	0.026837840
Signature.8	0.021972256	0.000214536
Signature.9	0.013244725	0.003783440

COSMIC, Catalogue Of Somatic Mutations In Cancer; PanNENs, pancreatic neuroendocrine neoplasm; NP-NENs, nonpancreatic neuroendocrine neoplasm. The sum of 30 signatures is equal 1.

Table S3 Frequency of mutation and LOH of commonly altered genes in PanNENs and NP-NENs

Genes	Ref (12) (%)		Our data (%)	
	Mutation frequency	LOH frequency	Mutation frequency	LOH frequency
MEN1	41	70	6	30.6
DAXX	22	53	0	14.3
ATRX	10	19	6	13.3
PTEN	7	40	2	30.6
TP53	4	–	31	49.0
DEPDC5	2	49	2	38.8
MUTYH	6	47	2	10.2
CHEK2	4	49	0	38.8
BRAC2	1	9	0	44.9
SETD2	5	51	4	38.8
MLL3	5	10	–	–
TSC1	2	17	2	20.4
TSC2	2	43	8	28.6
RB1	2	–	6	53.1
BRAF	0	–	6	14.3
VHL	1	–	2	34.7

LOH, loss of heterozygosity; PanNENs, pancreatic neuroendocrine neoplasm; NP-NENs, nonpancreatic neuroendocrine neoplasm.

Table S4 Frequency of common arm-level copy number alteration in PanNENs and NP-NENs

Arm SCNA	Ref (38) (%)	Our data (%)
11q loss	39	26.5
6q loss	38	12.2
11p loss	34	20.4
3p loss	27	24.5
1p loss	28	8.2
10q loss	26	30.6
1q loss	24	2.0
17q gain	41	12.2
7q gain	35.90	12.2
20q gain	30.70	24.5
9p gain	19.20	12.2
7p gain	28	20.4
9q gain	26.90	16.3

PanNENs, pancreatic neuroendocrine neoplasm; NP-NENs, nonpancreatic neuroendocrine neoplasm; SCNA, somatic copy number alteration.

Table S5 Cox multivariate analysis with several factors and OS

Variables	HR	95% CI	P
CIN *vs.* CS	15.06	1.01–224.71	0.049
NEC *vs.* NET	1.52	0.06–40.63	0.802
Male *vs.* female	1.28	0.18– 9.19	0.804
Age (numeric)	1.02	0.94–1.12	0.617

OS, overall survival; CIN, chromosomal instability; CS, chromosomal stable; NEC, neuroendocrine carcinoma; NET, neuroendocrine tumor; HR, hazard ratio; 95% CI, 95% confidence interval.